

Phase transitions of the random-bond Potts chain with long-range interactions

Jean-Christian Anglès d'Auriac¹ and Ferenc Igloi^{2,3,*}

¹*Institut Néel-MCBT CNRS, B. P. 166, F-38042 Grenoble, France*

²*Wigner Research Centre, Institute for Solid State Physics and Optics, H-1525 Budapest, P.O.Box 49, Hungary*

³*Institute of Theoretical Physics, Szeged University, H-6720 Szeged, Hungary*

(Received 26 July 2016; published 19 December 2016)

We study phase transitions of the ferromagnetic q -state Potts chain with random nearest-neighbor couplings having a variance Δ^2 and with homogeneous long-range interactions, which decay with distance as a power $r^{-(1+\sigma)}$, $\sigma > 0$. In the large- q limit the free-energy of random samples of length $L \leq 2048$ is calculated exactly by a combinatorial optimization algorithm. The phase transition stays first order for $\sigma < \sigma_c(\Delta) \leq 0.5$, while the correlation length becomes divergent at the transition point for $\sigma_c(\Delta) < \sigma < 1$. In the latter regime the average magnetization is continuous for small enough Δ , but for larger Δ —according to the numerical results—it becomes discontinuous at the transition point, thus the phase transition is expected of mixed order.

DOI: [10.1103/PhysRevE.94.062126](https://doi.org/10.1103/PhysRevE.94.062126)

I. INTRODUCTION

The properties of phase transitions in a pure system can be modified due to quenched disorder. This problem has been studied in detail at a second-order (SO) transition point [1,2], but much less is known when the transition is of first order [3]. When the disorder is coupled to the local energy density, such as for bond disorder, there is a general tendency that the latent heat at the transition point is reduced [4]. In two-dimensional systems with nearest-neighbor [or short-range (SR)] interactions, any amount of bond disorder is enough to turn the transition into second order [5]. The new universality class of the problem, however, remains unknown and numerical investigations are needed to identify the properties of the emergent random fixed point [6–10]. In three- and higher-dimensional SR systems, however, weak disorder is generally irrelevant, thus the phase-transition stays discontinuous and only for strong-enough disorder will it turn to a second-order one. This type of problem has been numerically studied for the q -state Potts model with $q > 2$ [11–15]. In particular a mapping between the random-field Ising model (RFIM) and the Potts model in the $q \rightarrow \infty$ limit has been used to predict some tricritical exponents of the latter random model [7,15].

Homogeneous, i.e., nonrandom systems with long-range (LR) interactions could have an ordered phase [16] and a first-order transition, too, even if the system is one dimensional. This happens, among others, for the q -state Potts chain [17] with power-law interactions

$$J(r) \approx Jr^{-(1+\sigma)}, \quad (1)$$

where r is the distance between the sites and the exponent is $\sigma > 0$ to have extensive total energy (for $\sigma < 0$ one should divide J by $L^{|\sigma|}$). According to numerical results [18] the transition in the LR Potts chain is of first order for sufficiently large values of q , where the limiting value $q_c = q_c(\sigma)$ is an increasing function of σ . On the other hand, the transition for $q < q_c(\sigma)$ is of second order.

Low-dimensional LR models with power-law interactions became the subject of intensive research recently, after it was noticed that the decay exponent σ in the problems plays the role of some kind of effective dimensionality of the analogous SR model. Among the classical problems studied so far we mention the nonrandom Ising model in one and two dimensions [19–23], the nonrandom Potts chain [18], the Ising spin-glass model [24–27], and the RFIM in one dimension [28–35]. For quantum models we mention investigations of the transverse-field Ising model both with pure [36–46] and random couplings [47–50] and the Anderson localization problem [51], for reaction-diffusion type models the contact process and similar models with [49] and without [52–61] quenched disorder.

The critical properties of LR models are often unusual. Here we mention that the classical Ising chain for $\sigma = 1$, as well as other one-dimensional discrete spin models with LR interaction have a so-called mixed-order (MO) phase transition [62–68], at which point the order-parameter has a jump, but at the same time the correlation length is divergent. We note that recently MO transitions have been observed in other problems, too [50,69–83].

In the present paper we consider LR models having a first-order transition in their nonrandom version and study the effect of quenched disorder on the phase-transition properties of the system. To be specific, we consider the LR Potts model in one dimension for large values of q (actually we consider the $q \rightarrow \infty$ limit), when the transition of the pure model is of first order for all values of the decay exponents, $\sigma > 0$. We have random nearest-neighbor couplings with a variance Δ^2 , but the long-range forces are nonrandom and follow the behavior in Eq. (1). We study the phase transition of the system for different values of the effective dimensionality σ and the strength of disorder Δ . The free energy and the magnetization of a given random sample is calculated exactly by a computer algorithm, which works in a time polynomial in the number L of spins [84]. We follow the temperature dependence of the average magnetization in relatively large finite samples and the location of the phase-transition point and its properties are analyzed by finite-size extrapolation methods.

*igloi.ferenc@wigner.mta.hu

The structure of the paper is the following: The model and some results are summarized in Sec. II. Numerical results at different points of the phase diagram are presented in Sec. III and analyzed by finite-size scaling. We close our paper with a discussion in Sec. IV.

II. MODEL AND SOME RESULTS

We consider the ferromagnetic q -state Potts model [17] in a one-dimensional periodic lattice with long-range interactions defined by the Hamiltonian

$$\mathcal{H} = - \sum_i J_i \delta(s_i, s_{i+1}) - \sum_{i < j+1} J_{ij} \delta(s_i, s_j). \quad (2)$$

Here $s_i = 1, 2, \dots, q$ is a Potts-spin variable at site $i = 1, 2, \dots, L$ and the long-range interaction J_{ij} has a power-law dependence as in Eq. (1) with $r = \min(L - |i - j|, |i - j|)$. The nearest neighbor couplings $J_i \equiv J_{i, i+1}$ are random variables. For simplicity we take J_i from a bimodal distribution, being either $J_- = J - \Delta$ or $J_+ = J + \Delta$ with equal probability. In the following we set the energy scale to $J = 1$ and restrict ourselves to $0 < \Delta < 1$.

A. The large- q limit

In this paper we consider the $q \rightarrow \infty$ limit of the model, when the reduced free energy in the Fortuin–Kasteleyn representation [85] is dominated by a single graph [86], the so-called optimal graph G , and is given by

$$-\beta f L = \max_G W(G), \quad W(G) = \left[c(G) + \beta \sum_{ij \in G} J_{ij} \right]. \quad (3)$$

Here $c(G)$ stands for the number of connected components of G and $\beta = 1/(T \ln q)$, with the temperature T .

In the *homogeneous nonrandom model* with $\Delta = 0$ there are only trivial optimal graphs as shown in Appendix A for any σ . In the low-temperature phase, $T < T_c$, it is the fully connected graph G_c with $W(G_c) = -\beta L f_{\text{hom}} = 1 + L\beta \mathcal{Z}_L(1 + \sigma)$, with

$$\begin{aligned} \mathcal{Z}_L(1 + \sigma) &= \frac{1}{L} \sum_{i=1}^{L/2} (L + 1 - i) i^{-(1+\sigma)} \\ &= \left(1 + \frac{1}{L}\right) \zeta_{L/2}(1 + \sigma) - \frac{1}{L} \zeta_{L/2}(\sigma), \end{aligned} \quad (4)$$

where we have assumed that L is *even*. Here $\zeta_{L/2}(\alpha) = \sum_{i=1}^{L/2} i^{-\alpha}$ and for $L \rightarrow \infty$ we have the Riemann zeta function $\zeta(\alpha)$. In the high-temperature phase $T > T_c$, the optimal graph is the empty graph G_e with $W(G_e) = -\beta L f_{\text{hom}} = L$. The phase-transition point in the thermodynamic limit is given by $\beta_c = 1/\zeta(1 + \sigma)$ where the phase transition is of first order having the maximal jump in the magnetization.

In the limit where σ goes to infinity one recovers the disordered SR Potts chain. In that case and for finite-size L , there are nontrivial optimal sets. But in the thermodynamical limit, the magnetization still jumps from zero to one for the bimodal distribution. This is shown in the Appendix A.

B. Stability analysis of the random model

Here we start with weak disorder, $\Delta \ll 1$, and estimate the characteristic function of nonhomogeneous optimal graphs. First let us consider an island of $l + 1 \leq \frac{L}{2}$ consecutive sites, which are fully connected within the sea of isolated points. The corresponding characteristic function is given by (see Appendix B)

$$W(G_1) = L - l + \beta[(l + 1)\zeta_l(1 + \sigma) - \zeta_l(\sigma)] + \beta \Delta \epsilon(l), \quad (5)$$

where $\epsilon(n)$ is the sum of n random numbers with mean zero and variance unity, thus $\epsilon(n) \sim \sqrt{n}$ for large n . At the transition point of the pure system, $\beta = \beta_c = 1/\zeta(1 + \sigma)$, the new diagram is the optimal set, i.e., $W(G_1) > W(G_e)$, provided $\Delta > \{l[\zeta(1 + \sigma) - \zeta_{l-1}(1 + \sigma)] + \zeta_l(\sigma)\}/\epsilon(l - 1)$. For large l the right-hand side (r.h.s.) of this inequality scales as $l^{1-\sigma}/l^{1/2} \sim l^{1/2-\sigma}$, thus we have the condition

$$\Delta > C l^{1/2-\sigma}, \quad l \gg 1. \quad (6)$$

Consequently, for a decay exponent $\sigma > 1/2$ there is a new, nonhomogeneous optimal set and the (phase-transition) properties of the system are modified by any small amount of disorder, at least in the thermodynamic limit. On the contrary for $\sigma < 1/2$ the transition, at least for small Δ , stays first order and could be changed only by strong-enough disorder, i.e., for large Δ .

Next we study the stability of the fully connected graph G_c and consider a diagram, G_2 , in which in a fully connected sea of points there are l disconnected sites. Its characteristic function is given by (see Appendix B)

$$\begin{aligned} W(G_2) &= l + 1 + \beta L \mathcal{Z}_L(1 + \sigma) \\ &\quad - \beta \{l[2\zeta_{L/2}(1 + \sigma) - \zeta_l(1 + \sigma)] + \zeta_l(\sigma)\} \\ &\quad + \beta \Delta \epsilon(l + 1). \end{aligned} \quad (7)$$

At $\beta = \beta_c$ we have $W(G_2) < W(G_c)$, at least for weak disorder for any value of $\sigma > 0$. This means that, considering the stability of the two trivial optimal sets of the pure system at $\beta = \beta_c$, these are not symmetric. For $\sigma > 1/2$ the empty diagram is unstable, while the fully connected graph is stable for weak disorder. We note that, in the SR model, both graphs become unstable at the same value of the dimensionality, $d \leq 2$.

In the LR model in the modified transition regime, $\sigma > 1/2$, we can define a breaking-up length:

$$l^* \sim \Delta^{1/(1/2-\sigma)}, \quad \sigma > 1/2, \quad (8)$$

which is the typical size of connected clusters. This means that, in a finite system, one should have $L > l^*$ to be able to observe a new type of transition, otherwise there is a pseudo-first-order transitions in the finite system.

C. Relation with the random-field Ising model

The previous stability analysis is based on the properties of an interface separating the two trivial optimal graphs, and analogous reasoning due to Imry and Ma [87] works for the RFIM, in which case the interface separates the ordered and disordered regions of the model. This mapping has been

observed by Cardy and Jacobsen [7] and can be generalized for LR interactions, in which case the RFIM in a one-dimensional lattice is defined by the Hamiltonian

$$\mathcal{H}_{\text{RFIM}} = - \sum_i B_i S_i - \sum_{i<j} J_{ij} S_i S_j, \quad (9)$$

in terms of $S_i = \pm 1$. Here B_i is a random variable with zero mean and variance Δ^2 , and J_{ij} is in the same form as in Eq. (1). The critical behavior of $\mathcal{H}_{\text{RFIM}}$ has been studied in the literature [28–35] and σ -dependent properties are found, which are summarized in the following.

There is a ferromagnetic ordered phase in the system for $0 < \sigma < 1/2$ [which corresponds to phase coexistence, i.e., a first-order transition in the random-bond Potts model (RBPM)] and there is no spontaneous ordering for $\sigma > 1/2$ (which is analogous to the absence of a first-order transition in the RBPM). The transition to the ferromagnetic ordered phase is mean-field (MF) type in the region $0 < \sigma < 1/3$, where the critical exponents are the MF ones: $\alpha_{\text{RF}} = 0$, $\beta_{\text{RF}} = 1/2$, $\gamma_{\text{RF}} = 1$, and $\nu_{\text{RF}} = 1/\sigma$. On the contrary for $1/3 < \sigma < 1/2$ the transition is non-MF: the critical exponent ν_{RF} is not known exactly, but we have the relations

$$\frac{2 - \alpha_{\text{RF}}}{\nu_{\text{RF}}} = 1 - \sigma, \quad \frac{\beta_{\text{RF}}}{\nu_{\text{RF}}} = \frac{1}{2} - \sigma, \quad \frac{\gamma_{\text{RF}}}{\nu_{\text{RF}}} = \sigma. \quad (10)$$

Cardy and Jacobsen [7] have conjectured relations between the magnetization exponents of the RFIM and the tricritical exponents in the energy sector of the RBPM, at least for SR models. If we assume the validity of these relations for LR interactions, too, we have for the correlation-length exponent of the RBPM at the tricritical point:

$$\nu = \frac{\nu_{\text{RF}}}{\beta_{\text{RF}} + \gamma_{\text{RF}}}. \quad (11)$$

Thus the conjectured results are $\nu = \frac{2}{3\sigma}$ and $\nu = 2$ in the MF-region and in the non-MF region, respectively.

III. NUMERICAL CALCULATION

A. Preliminaries

As for systems with quenched disorder one should perform two averages: first, the thermal average for a given realization of disorder and, second, averaging over the disorder realizations. For a given random sample of length L the thermal average is obtained through the solution of the optimization problem given in Eq. (3). Having the optimal graph of the sample, we have the free energy as well as the structure of connected clusters in this graph. The magnetization of the sample, m , is given by the number of sites in the largest cluster, N_{max} , as $m = N_{\text{max}}/L$. To study the properties of the phase-transitions in the system it is convenient to monitor the behavior of the average magnetization. In some cases, however, we have also studied the behavior of the average internal energy. The analyses of the average internal energy is more complicated, while in the case of bimodal disorder there are extra jumps; see Ref. [10]. The optimization process for a given sample is solved exactly by a combinatorial optimization algorithm which works in a time polynomial in the number L of spins [84]. This makes it possible to treat relatively large samples up to $L = 1024$ and in some cases up to $L = 2048$.

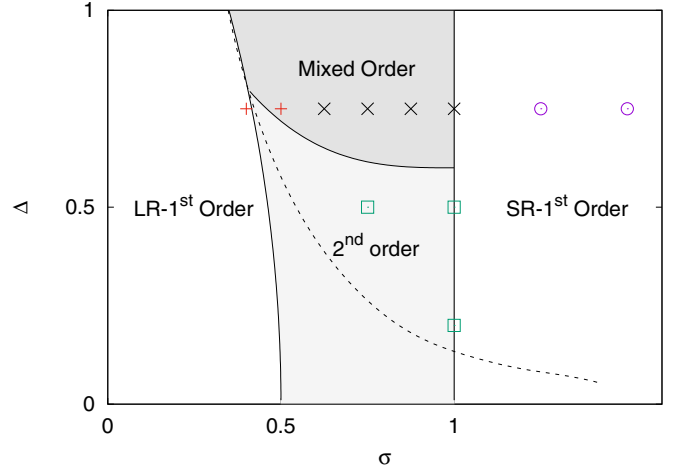


FIG. 1. Schematic phase-diagram of the LR Potts chain with random nearest-neighbor couplings in the $q \rightarrow \infty$ limit together with points of the phase diagram studied numerically. The border of the strongly first-order regime in a finite system (dashed line) is calculated with $L = 256$ and with $N^\# = 600$ samples. In the area to the left of this border in such a finite system the transition is between the fully connected graph and the empty graph; see the text. The plus sign refers to long-range first-order transitions, the cross sign refers to mixed-order transitions, the circle to short-range first-order transitions, and the square to second-order transitions.

In the latter case the typical computational time of a sample in the complete temperature range is about 6 to 7 hours with a 2.4 GHz processor. A drawback of the calculation is that the possible graphs in the present problem are fully connected, having $L(L-1)/2$ possible edges and the algorithm needs so many iterations, which increases the computational time accordingly. In the second step of the averaging process we have considered several independent random samples, their typical number being a few 10 000, for $L = 1024$ a few 1000.

B. Magnetization profiles

Before entering into the details to study the phase-diagram of the system, we make a rough estimate of the domain, in which the transition is very strongly first order, at least for the finite systems, we can use in the numerical calculation. For this purpose we analyzed the phase transition of $N^\# = 600$ random samples of length $L = 256$. In Fig. 1 there is dashed line, which indicates the border obtained by this analysis. In the area to the left of this border in all samples the transition is between the fully connected graph and the empty graph; thus, the transition is maximally first order, as in the homogeneous system. By increasing L , this border is expected to be shifted to the left and in the thermodynamic limit it stays inside of the phase labeled by “LR-1st order” of the phase diagram in Fig. 1. Next, we have chosen several points outside the strongly-first-order regime, i.e., to the right of the dashed line, which are indicated in Fig. 1. The selected points can be divided into two groups: a set of points with relatively weak disorder, $\Delta = 0.2$ and $\Delta = 0.5$ and another set with quite strong disorder, $\Delta = 0.75$. At each point the calculation of the optimal graph is performed in the complete temperature range: we have monitored the temperature dependence of the

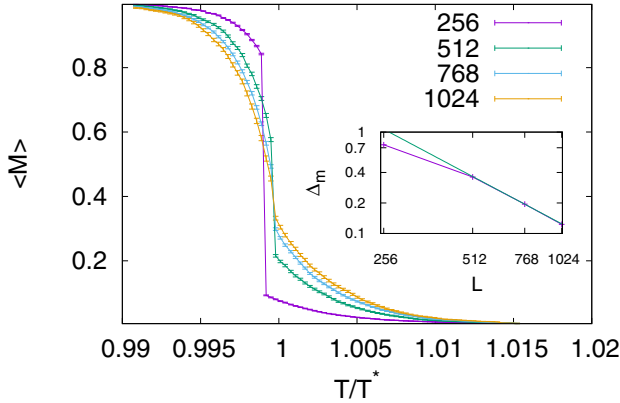


FIG. 2. Finite-size magnetizations at $\Delta = 0.2$ and $\sigma = 1$. In the inset the magnetization jump at the transition point is shown as a function of the size of the system on a log-log scale. The straight green line has a slope $\beta/\nu \approx 1.55$.

magnetization and focused on its possible singular behavior. These calculations are performed in finite systems with $L = 64, 128, \dots, 1024$ and the actual properties of the singularity, thus the form of the phase transition is analyzed by finite-size extrapolation. To make all the figures easily comparable we have normalized the temperature by $T^* = 1/\beta_c$, which is the sum of all the coupling constants; see Sec. II A.

1. Weak and intermediate disorder regimes: $\Delta = 0.2$ and 0.5

For weak disorder with $\Delta = 0.2$ we studied the point of the phase-diagram with $\sigma = 1$ (square in Fig. 1), i.e., at border of the LR regime. The magnetization profiles are shown in Fig. 2. It is seen that, due to disorder, the first-order transition in the pure system is rounded: the jump in the magnetization decreases with increasing size, and in the thermodynamic limit the jump is expected to disappear, $\Delta m(L) \sim L^{-\beta/\nu}$, so that the limiting curve $\lim_{L \rightarrow \infty} m(L, T) = m(T)$ is continuous. However, its derivative at $T = T_c$ is expected to be divergent, so that $m(T) - m(T_c) \sim |T - T_c|^\beta$. The finite-size transition points are expected to be shifted as $T_c - T_c(L) \sim L^{-1/\nu}$. Note that,

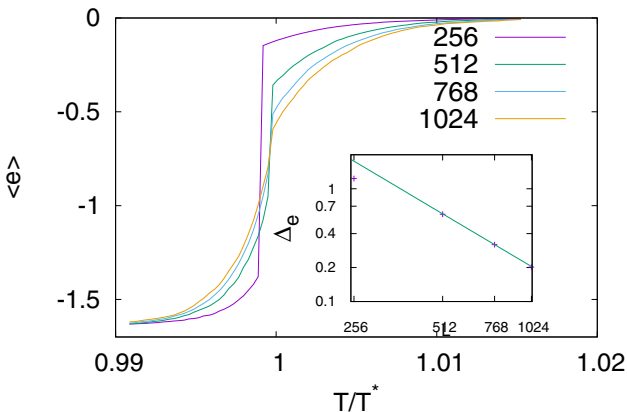


FIG. 3. Average energy for finite systems at $\Delta = 0.2$ and $\sigma = 1$. In the inset the finite-size latent heats (jumps of the energy at the transition point) are shown for different sizes on a log-log scale. The straight green line has a slope $(1 - \alpha)/\nu \approx 1.55$.

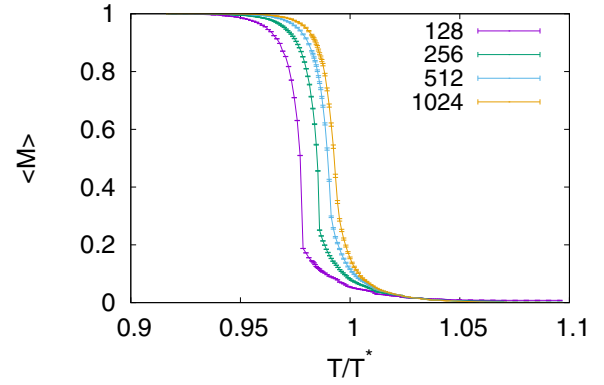


FIG. 4. Second-order transition at $\Delta = 0.5$ and $\sigma = 0.75$.

for $T < T_c$ ($T > T_c$), the profiles satisfy $m(L_1, T) > m(L_2, T)$ [$m(L_1, T) < m(L_2, T)$] for $L_1 < L_2$. With the numerical data in Fig. 2 we could not estimate ν since the transition point T_c is not known with sufficient precision. However, we could analyze the size dependence of the magnetization jump; see inset of Fig. 2, and we obtained an exponent $\beta/\nu \approx 1.55$. Note that the mean-field value is $\beta/\nu = 1$. We should mention that, according to the numerical data in Fig. 2, the magnetization seems to approach a finite limiting value above the transition temperature. This could be an artifact, that the calculation is performed in the case $q \rightarrow \infty$ and for finite values of q we probably recover the expected vanishing of the magnetization for $T > T_c$ (see also the remark in Sec. III B 2 c). We also studied the temperature dependence of the average energy density, which is shown in Fig. 3. At the transition point in small finite systems there is a discontinuity of the energy density, $\Delta e(L)$, which seems to disappear in the thermodynamic limit as $\Delta e(L) \sim L^{-(1-\alpha)/\nu}$, but its first derivative, the specific heat, is divergent: $C(T) \sim |T - T_c|^{-\alpha}$. The finite-size behavior of $\Delta e(L)$ is shown in the inset of Fig. 3; see the very similar behavior as the magnetization jump in the inset of Fig. 2. We obtained an estimate $\alpha/\nu \approx -0.55$ and thus a relation $\beta + \alpha \approx \nu$ is noticed at this point. Thus we conclude that the transition according to the Ehrenfest classification is of second order.

For intermediate disorder, $\Delta = 0.5$, two points are considered with $\sigma = 0.75$ and $\sigma = 1.0$, the calculated average

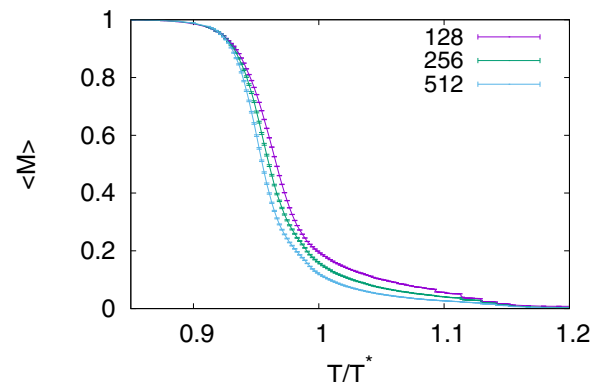


FIG. 5. Magnetization for $\Delta = 0.5$ and at the border $\sigma = 1$.

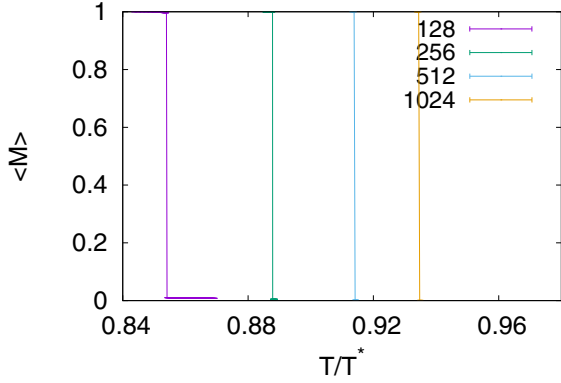


FIG. 6. First-order transition due to LR forces at $\Delta = 0.75$ and $\sigma = 0.4$.

magnetization profiles are presented in Figs. 4 and 5. In both cases the transition seems to be of second order, which is in agreement with the temperature dependence of the energy densities.

2. Strong-disorder regime: $\Delta = 0.75$

At the disorder parameter $\Delta = 0.75$ we studied different regimes by varying the decay exponent σ .

a. $\sigma \lesssim 0.5$: Long-range first-order transitions. See plus signs in Fig. 1. At the point $\sigma = 0.4$ in Fig. 6 the average magnetization has a finite jump of $\Delta m \approx 1$ for all finite systems. The finite-size transition points, which are identified with the position of the jump, $T_c(L)$, are shifted such that $T_c(L_1) < T_c(L_2)$ for $L_1 < L_2$. Furthermore, the distance from the true transition point is well described by the asymptotic behavior in the nonrandom system: $\Delta T_c = T_c - T_c(L) \sim L^{-\sigma}$, since $T_c(L) \propto \text{cst} \zeta_L(1 + \sigma)$. Thus the scaling exponent associated with lengths is $\nu \approx 1/\sigma$. At this point, and in general, in the regime $\sigma \lesssim 0.5$ there is a *random first-order transition* due to LR forces.

At the borderline value of $\sigma = 0.5$ the magnetization profiles in Fig. 7 still show a jump, at least for smaller finite systems. With increasing L , however, the jump in the magnetization is going to be rounded, so that the transition could be continuous in the thermodynamic limit.

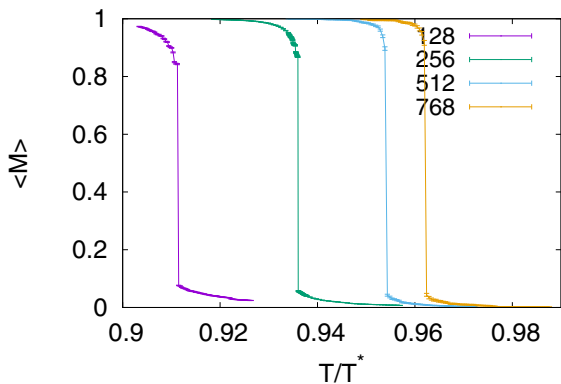


FIG. 7. The jump in the magnetization is rounded due to disorder at $\Delta = 0.75$ and $\sigma = 0.5$.

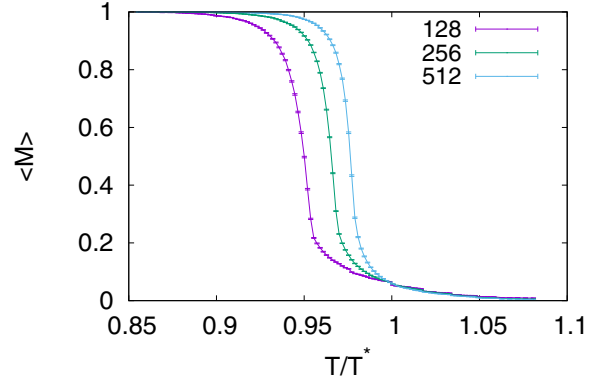


FIG. 8. Mixed-order transition at $\Delta = 0.75$ and $\sigma = 0.625$.

With the finite-size results at hand we cannot discriminate between these scenarios. The shift of the finite-size transition points are characterized by an exponent $\nu \approx 2 = 1/\sigma$ in this case, too.

b. $0.5 < \sigma \leq 1.0$: Mixed-order transitions. See crosses in Fig. 1. In this regime we have a series of points with $\sigma = 0.625, 0.75, 0.875$, and 1.0 and the corresponding profiles are shown in Figs. 8–11. The new feature of the profiles is that, for different sizes, they cross each other, so that for $T < T_c$ ($T > T_c$) the profiles satisfy $m(L_1, T) < m(L_2, T)$ [$m(L_1, T) > m(L_2, T)$] for $L_1 < L_2$. From this we expect (if the L dependence stays monotonic and no reversal of the tendency will be found for larger values of L) that at the transition point in the thermodynamic limit the magnetization has a finite limiting value: $\lim_{L \rightarrow \infty} m(L, T_c^-) = m^- > 0$, which is different from the limit $\lim_{L \rightarrow \infty} m(L, T_c^+) = m^+$. Consequently at the transition point there is a jump in the magnetization: $\Delta m = m^- - m^+$. We also expect that the actual value of m^+ is (close to) zero for strong disorder (large Δ) and it is increasing for smaller values of Δ . In the thermodynamic limit for $T < T_c$ the magnetization is expected to follow a singular temperature dependence: $m(T) - m^- \sim (T_c - T)^\beta$. This can be checked in finite systems by defining finite-size transition points as the crossing points of the profiles $m(L_1, T)$ and $m(L_2, T)$: $m[L_1, T_c(L_1, L_2)] = m[L_2, T_c(L_1, L_2)] \equiv m^-(L_1, L_2)$. According to scaling

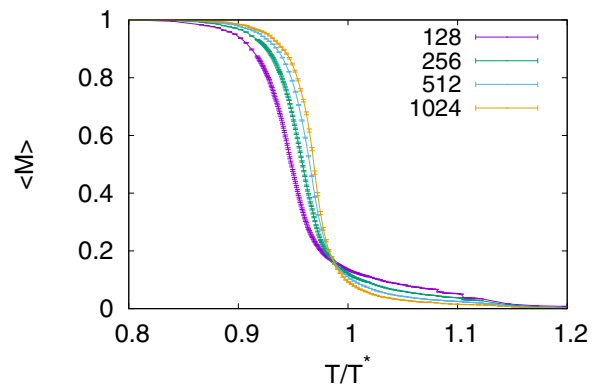
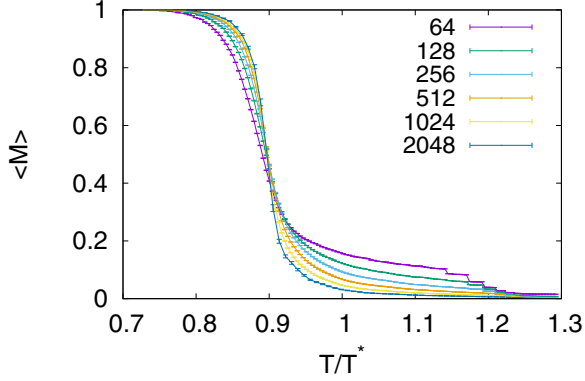


FIG. 9. Mixed-order transition at $\Delta = 0.75$ and $\sigma = 0.75$.


 FIG. 10. Mixed-order transition at $\Delta = 0.75$ and $\sigma = 0.875$.

theory the differences should behave asymptotically as $T_c(L_1, L_2) - T_c \sim (L_1 L_2)^{-\frac{1}{2\nu}}$ and $m^- - m^-(L_1, L_2) \sim (L_1 L_2)^{-\frac{\beta}{2\nu}}$. Due to strong finite-size corrections we could make an estimate for the critical exponents only at the point $\sigma = 0.875$, in which case the measured quantities are presented in Table I.

From these data we obtain the following estimates for the exponents: $1/\nu \approx 1.27$ and $\beta/\nu \approx 0.78$. This means that, at this point, or more generally in the $0.5 < \sigma \leq 1.0$ part of the phase diagram (with $\Delta = 0.75$), there is a mixed-order phase transition in the system: the magnetization has a jump at the transition point, but the correlation length is divergent at T_c .

Comparing the magnetization profiles at different values of σ , one can notice that its limiting value m^- and thus the jump Δm is an increasing function of σ in the given range. Increasing σ over the upper limit, $\sigma = 1$, the form of the singularity changes once more.

c. $\sigma > 1.0$: Short-range first-order transitions. See circles in Fig. 1. The magnetization profiles at $\sigma = 1.25$ and 1.5 in Figs. 12 and 13 show similar features: a jump develops for large L , the asymptotic position of which is at $T_c(\sigma)/\zeta(1 + \sigma) < 1$, which ratio is decreasing with increasing σ and in the true SR model with $\sigma \rightarrow \infty$ this ratio is just $1 - \Delta$. Thus in this region the transition is of first order due to SR interactions. Comparing the finite-size transition temperatures $T_c(L)$, defined as the inflection point of the profiles, we observe the asymptotic behavior $T_c(L) - T_c \sim L^{-1}$, which is characteristic for SR

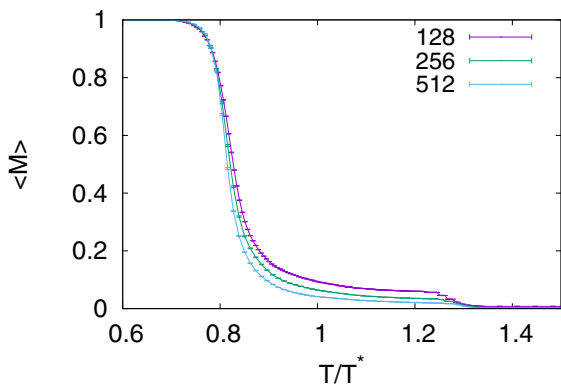

 FIG. 11. Magnetization for $\Delta = 0.75$ and at the border $\sigma = 1$.

 TABLE I. Finite-size parameters of the transition point for $\Delta = 0.75$ and $\sigma = 0.875$. In the last row the extrapolated values are presented.

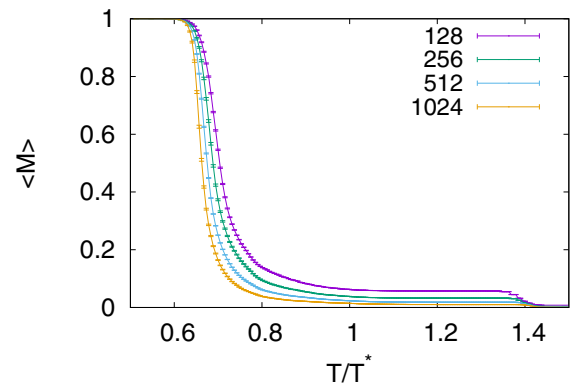
L_1	L_2	$T_c(L_1, L_2)$	$m^-(L_1, L_2)$
128	256	0.9118	0.3389
256	512	0.8985	0.4879
512	1024	0.8930	0.5745
		0.8894	0.695

forces. We note that spontaneous order in the LR Potts chain for $\sigma > 1$ can be observed only in the $q \rightarrow \infty$ limit. For any finite value of q due to thermal fluctuations there is no ordered phase, thus the SR first-order transition regime is absent.

IV. DISCUSSION

We have studied numerically the phase diagram of the ferromagnetic LR Potts chain with random nearest-neighbor couplings in the $q \rightarrow \infty$ limit. We expect that the trends observed in finite samples represent the asymptotic behavior and no reversal of the tendency will be found for larger values of L . Depending on the strength of disorder Δ and the decay exponent σ , different type of phase transitions are found: first-order transitions due to LR interactions, first-order transitions due to SR interactions, second-order transitions, and mixed-order transitions. A schematic phase diagram is depicted in Fig. 1.

For small values of $\sigma < \sigma_c(\Delta) \leq 0.5$ the long-range interactions are dominant over quenched disorder and the transition is of first order, as in the nonrandom system. For large values of $\sigma > 1$ the transition is also of first order; however, now due to short-range interactions. We note that, for finite values of q in this region, there is no ferromagnetic order in the system. For intermediate values of the decay exponent $\sigma_c(\Delta) < \sigma < 1$, quenched disorder is going to change the order of the transition. For weaker disorder the transition turns to second order, which is manifested by a divergent specific heat and by a divergent correlation length; however, the magnetization at the critical point is continuous and has a finite value. For strong disorder the transition turns out to be of mixed order. At the transition point the correlation length is divergent, but there is a finite


 FIG. 12. First-order transition due to SR forces at $\Delta = 0.75$ and $\sigma = 1.25$.

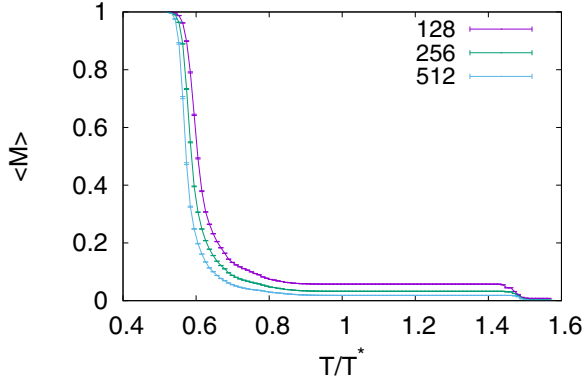


FIG. 13. First-order transition due to SR forces at $\Delta = 0.75$ and $\sigma = 1.5$.

jump in the magnetization, as well as in the energy density. The finite-size scaling behavior of the magnetization profiles are also different in the SO and the MO transitions.

The different type of transitions are connected with the geometric properties of the optimal graphs. At first-order transitions, the optimal graphs are different at the two sides of the transition points: in the ferromagnetic phase there is a giant cluster, whereas in the high-temperature phase the clusters have finite mass and extent. At the second-order transition at both sides there is a giant cluster; however, at the transition a hole in this giant cluster is developed, the size of which as well as its mass are divergent. This hole in the SO transition point is a fractal, so the average magnetization is continuous. Similar process takes place at a mixed-order transition, too, with the difference that, in this case the “hole” in the high-temperature phase is a compact object having a finite density of mass. This leads to a jump in the magnetization in the thermodynamic limit. For large-enough Δ this hole is going to disconnect the giant cluster, so that the density of its mass, being the magnetization, has a vanishing value in the thermodynamic limit.

We expect that the results summarized in the phase diagram in Fig. 1 remain qualitatively correct for other, more general models, too. First we mention that the LR forces in Eq. (2) can be (weakly) random, too, which means that, in Eq. (1), the prefactor is modified as $J \rightarrow J_i$, and $J_i > 0$ are random variables. Another set of models are obtained if the parameter q is a large but finite value. As noted before this model for $\sigma > 1$ has no ordered phase; however, a similar phase diagram is expected to hold in the regime $0 < \sigma < 1$. This conjecture is based on the known results in the SR models, in which the properties of the phase transitions in different dimensions are found to be a smooth function of q , so that the $q \rightarrow \infty$ limit is not singular [8–10]. Further numerical work is needed to clarify if a similar relation also holds for the LR model.

ACKNOWLEDGMENTS

This work was supported by the Hungarian Scientific Research Fund under Grants No. K109577 and No. K115959. J-Ch. A.d’A. extends thanks to the “Theoretical Physics Workshop” and F.I. to the Université Joseph Fourier for supporting their visits to Budapest and Grenoble, respectively.

APPENDIX A

In this appendix we calculate exactly the free energy on the two lines $\Delta = 0$ and $\sigma \rightarrow \infty$ of the phase diagram. As explained in Ref. [84], finding the free energy amounts to finding the so-called optimal set. Let us recall that an optimal set is a set of edges that maximizes the objective function

$$f(S; \beta) = c(S) + \beta \sum_{e \in S} J(e),$$

where $c(S)$ is the number of connected components of S and β is the inverse temperature.

For any sample, the optimal set for zero temperature is the set of all bonds, while for high temperature the optimal set is empty. Between these two limits the optimal set changes at a finite number n_T of temperatures ($n_T < L$). We call these temperature “breaking temperatures.” If there is only one breaking temperature ($n_T = 1$) the model is maximally first order since the magnetization jumps from zero to one.

Let us first consider the case $\Delta = 0$: a nondisordered model. We show below that, for any decreasing weight function of distance (such as, for example, $d^{-(1+\sigma)}$) there is a single breaking temperature for any size L . Note first that, if a bond of length d , belongs to an optimal set, then there is an optimal set to which *all* bonds of length d are present. Indeed, the permutation of the sites $i \rightarrow i + 1$ preserve the length of the bonds and therefore any bonds of length d belongs to some optimal set. The union of two optimal sets is also an optimal set as shown in Ref. [84], this is the property which makes polynomial this problem. Therefore, we deduce that there is an optimal set to which all bonds of length d belong. Suppose now that the bond between site 0 and site d belongs to the optimal set. Then the bond between the sites d and $2d$ also belongs to the optimal set and consequently the site 0, d , $2d$ belongs to the same cluster. More generally all the bonds between αd and $(\alpha + 1)d$ also belong to the optimal set and consequently all sites αd , where the product is modulo L and α an arbitrary integer, belong to the same cluster. If L is a prime number, then all the sites will be attained, and therefore the optimal set contains all bonds if it contains any one bond, which proves the results. Note that, in this special case of L being prime, we did not use the fact that the weight function is decreasing. To sketch the results in the case where $L = ln$ is not a prime number we introduce the sets of edges $C_{n,l}(k)$ induced by the vertex sets $\{k, l + k, 2l + k, \dots, (n-1)l + k\}$. It is clear that every optimal set is of the form $R(n) = \bigcup_{k=0}^{l-1} C_{n,l}(k)$ and is therefore characterized by a divisor of L . Showing that the transition is maximally first order amounts to showing that the optimal set is characterized by only either 1 or L . To this end, let us introduce the sets of edges $\Gamma_n(k)$ induced by the set of vertices $\{k, k + 1, \dots, k + (n-1)\}$. A union $S(n) = \bigcup_{k=0}^{l-1} \Gamma_n(nk)$ is in general not an optimal set. However, comparing the objective function for $S(n)$ and $R(n)$ and using the fact that J is a decreasing function of the distance, we find that only $S(1)$ and $S(L)$ can be the optimal set. This proves that the model is maximally first order also when L is not prime.

Now we turn to the case $\sigma \rightarrow \infty$, i.e., when only the short-range disordered bonds are present. In the general case the coupling constant can take n values $0 < J_0 \leq J_1 \leq \dots \leq J_{n-1}$ the breaking temperatures $T_k = \frac{1}{k-1} \sum_{i=0}^{L-1} J_i$ for $2 \leq k \leq L$.

Using this relation in the case of bimodal distribution with an equal number of strong $(1 + \Delta)$ and weak $(1 - \Delta)$ bonds, one gets $1 - \Delta = J_0 = \dots = J_{\frac{l}{2}} < J_{\frac{l}{2}+1} = \dots = J_{L-1} = 1 + \Delta$ from which the T_k are easily deduced. After some algebra one gets that, if $\Delta \leq \frac{1}{L-1}$, the model is maximally first order with a breaking temperature $\frac{L}{L-1}$, while if $\frac{1}{L-1} < \Delta$ there are two breaking temperatures $T_1 = \frac{L}{L-2}(1 - \Delta)$ and $T_2 = 1 + \Delta$. In the intermediate regime $T_1 \leq \bar{T} \leq T_2$ the free energy is $f(T, L) = \frac{1}{2} + \frac{1}{2} \frac{1+\Delta}{T}$, and we have numerically observed that magnetization scales as $L^{-0.82}$. So in the thermodynamical limit the magnetization jumps from 0 to 1 at T_2 .

Note finally that *all* realizations have exactly the same behavior. Therefore, in some sense, the model is not disordered.

APPENDIX B

In this appendix we prove Eq. (5). The configuration G_1 is the set of the l bonds $(0,1), (1,2), \dots, (l, l+1)$. So the sites 0 to $l+1$ are in same connected components, while all others sites belong to a connected component of size 1 (singleton).

So there are $1 + (L - l + 1) = L - l$ connected components. Only the first connected component has a contribution to the sum of the weight of the bonds. This connected component has $l - d + 1$ pairs of sites at distance d , for d running from 1 to l and assuming $l + 1 < \frac{L}{2}$. We deduce that the sum of the nonrandom part of the weight of the bonds is

$$\sum_{d=1}^l (l - d + 1) \frac{1}{d^{1+\sigma}} = (l + 1) \sum_{d=1}^l \frac{1}{d^{1+\sigma}} - \sum_{d=1}^l \frac{1}{d^\sigma}.$$

Since $\zeta_l(\alpha) = \sum_{d=1}^l \frac{1}{d^\alpha}$, Eq. (5) follows.

The configuration G_2 can be seen as a configuration G_1 but with $l > \frac{L}{2}$. However, it is easier to see it as a complete graph from which appropriate bonds are removed. The formula in Eq. (7) is established in the very same way as the formula in Eq. (5). However, it is slightly more difficult, since from the complete graph one has to remove not only the bonds between the isolated sites (see the formula above), but also the bonds between the isolated sites and the $L - l$ sites of the large connected components.

-
- [1] A. B. Harris, *J. Phys. C: Solid State Phys.* **7**, 1671 (1974).
 [2] J. T. Chayes, L. Chayes, D. S. Fisher, and T. Spencer, *Phys. Rev. Lett.* **57**, 2999 (1986).
 [3] For a review, see J. Cardy, *Phys. A (Amsterdam, Neth.)* **263**, 215 (1999).
 [4] Y. Imry and M. Wortis, *Phys. Rev. B* **19**, 3580 (1979); K. Hui and A. N. Berker, *Phys. Rev. Lett.* **62**, 2507 (1989).
 [5] M. Aizenman and J. Wehr, *Phys. Rev. Lett.* **62**, 2503 (1989); **64**, 1311 (1990).
 [6] M. Picco, *Phys. Rev. Lett.* **79**, 2998 (1997); C. Chatelain and B. Berche, *ibid.* **80**, 1670 (1998); *Phys. Rev. E* **58**, R6899 (1998); **60**, 3853 (1999); T. Olson and A. P. Young, *Phys. Rev. B* **60**, 3428 (1999).
 [7] J. Cardy and J. L. Jacobsen, *Phys. Rev. Lett.* **79**, 4063 (1997); J. L. Jacobsen and J. Cardy, *Nucl. Phys. B* **515**, 701 (1998).
 [8] J. L. Jacobsen and M. Picco, *Phys. Rev. E* **61**, R13 (2000); M. Picco (unpublished).
 [9] J.-Ch. Anglès d'Auriac and F. Iglói, *Phys. Rev. Lett.* **90**, 190601 (2003).
 [10] M.-T. Mercaldo, J.-Ch. Anglès d'Auriac, and F. Iglói, *Phys. Rev. E* **69**, 056112 (2004).
 [11] K. Uzelac, A. Hasmy, and R. Jullien, *Phys. Rev. Lett.* **74**, 422 (1995).
 [12] H. G. Ballesteros, L. A. Fernández, V. Martín-Mayor, A. Muñoz Sudupe, G. Parisi, and J. J. Ruiz-Lorenzo, *Phys. Rev. B* **61**, 3215 (2000).
 [13] C. Chatelain, B. Berche, W. Janke, and P.-E. Berche, *Phys. Rev. E* **64**, 036120 (2001); W. Janke, P.-E. Berche, C. Chatelain, and B. Berche, *Nucl. Phys. B* **719**, 275 (2005).
 [14] M.-T. Mercaldo, J.-Ch. Anglès d'Auriac, and F. Iglói, *Europhys. Lett.* **70**, 733 (2005).
 [15] M.-T. Mercaldo, J.-Ch. Anglès d'Auriac, and F. Iglói, *Phys. Rev. E* **73**, 026126 (2006).
 [16] F. J. Dyson, *Commun. Math. Phys.* **12**, 91 (1969).
 [17] F. Y. Wu, *Rev. Mod. Phys.* **54**, 235 (1982).
 [18] Z. Glumac and K. Uzelac, *Phys. Rev. E* **58**, 4372 (1998); K. Uzelac and Z. Glumac, *Phys. Rev. Lett.* **85**, 5255 (2000); E. Bayong, H. T. Diep, and Viktor Dotsenko, *ibid.* **83**, 14 (1999); **85**, 5256 (2000).
 [19] M. E. Fisher, S. K. Ma, and B. G. Nickel, *Phys. Rev. Lett.* **29**, 917 (1972).
 [20] J. Sak, *Phys. Rev. B* **8**, 281 (1973).
 [21] E. Luijten and H. W. J. Blöte, *Phys. Rev. Lett.* **89**, 025703 (2002).
 [22] M. Picco, [arXiv:1207.1018](https://arxiv.org/abs/1207.1018); T. Blanchard, M. Picco, and M. A. Rajabpour, *Europhys. Lett.* **101**, 56003 (2013).
 [23] M. C. Angelini, G. Parisi, and F. Ricci-Tersenghi, *Phys. Rev. E* **89**, 062120 (2014).
 [24] G. Kotliar, P. W. Anderson, and D. L. Stein, *Phys. Rev. B* **27**, 602 (1983).
 [25] C. Monthus and T. Garel, *Phys. Rev. B* **89**, 014408 (2014).
 [26] C. Monthus and T. Garel, *J. Stat. Mech.* (2014) P03020.
 [27] C. Monthus, *J. Stat. Mech.* (2014) P06015.
 [28] A. J. Bray, *J. Phys. C: Solid State Phys.* **19**, 6225 (1986).
 [29] P. O. Weir, N. Read, and J. M. Kosterlitz, *Phys. Rev. B* **36**, 5760 (1987).
 [30] G. J. Rodgers and A. J. Bray, *J. Phys. A: Math. Gen.* **21**, 2177 (1988).
 [31] M. Aizenman and J. Wehr, *Commun. Math. Phys.* **130**, 489 (1990).
 [32] M. Cassandro, E. Orlandi, and P. Picco, *Commun. Math. Phys.* **288**, 731 (2009).
 [33] C. Monthus and T. Garel, *J. Stat. Mech.* (2011) P07010.
 [34] L. Leuzzi and G. Parisi, *Phys. Rev. B* **88**, 224204 (2013).
 [35] T. Dewenter and A. K. Hartmann, *Phys. Rev. B* **90**, 014207 (2014).
 [36] D. Porras and J. I. Cirac, *Phys. Rev. Lett.* **92**, 207901 (2004).

- [37] X. L. Deng, D. Porras, and J. I. Cirac, *Phys. Rev. A* **72**, 063407 (2005).
- [38] P. Hauke, F. M. Cucchietti, A. Müller-Hermes, M. Bañuls, J. I. Cirac, and M. Lewenstein, *New J. Phys.* **12**, 113037 (2010).
- [39] D. Peter, S. Müller, S. Wessel, and H. P. Büchler, *Phys. Rev. Lett.* **109**, 025303 (2012).
- [40] V. Nebendahl and W. Dür, *Phys. Rev. B* **87**, 075413 (2013).
- [41] M. L. Wall and L. D. Carr, *New J. Phys.* **14**, 125015 (2012).
- [42] S. A. Cannas and F. A. Tamarit, *Phys. Rev. B* **54**, R12661 (1996).
- [43] A. Dutta and J. K. Bhattacharjee, *Phys. Rev. B* **64**, 184106 (2001).
- [44] M. Dalmonte, G. Pupillo, and P. Zoller, *Phys. Rev. Lett.* **105**, 140401 (2010).
- [45] T. Koffel, M. Lewenstein, and L. Tagliacozzo, *Phys. Rev. Lett.* **109**, 267203 (2012).
- [46] P. Hauke and L. Tagliacozzo, *Phys. Rev. Lett.* **111**, 207202 (2013).
- [47] R. Juhász, I. A. Kovács, and F. Iglói, *Europhys. Lett.* **107**, 47008 (2014).
- [48] C. Monthus, *J. Stat. Mech.* (2015) P05026; (2015) P10024.
- [49] R. Juhász, I. A. Kovács, and F. Iglói, *Phys. Rev. E* **91**, 032815 (2015).
- [50] I. A. Kovács, R. Juhász, and F. Iglói, *Phys. Rev. B* **93**, 184203 (2016).
- [51] C. Monthus and T. Garel, *J. Stat. Mech.* (2010) P09015.
- [52] D. Mollison, *J. Roy. Stat. Soc. B* **39**, 283 (1977).
- [53] H. K. Janssen, K. Oerding, F. van Wijland, and H. J. Hilhorst, *Eur. Phys. J. B* **7**, 137 (1999).
- [54] H. Hinrichsen and M. Howard, *Eur. Phys. J. B* **7**, 635 (1999).
- [55] F. Ginelli, H. Hinrichsen, R. Livi, D. Mukamel, and A. Torcini, *J. Stat. Mech.* (2006) P08008.
- [56] C. E. Fiore and M. J. de Oliveira, *Phys. Rev. E* **76**, 041103 (2007).
- [57] F. Linder, J. Tran-Gia, S. R. Dahmen, and H. Hinrichsen, *J. Phys. A: Math. Theor.* **41**, 185005 (2008).
- [58] P. Grassberger, *J. Stat. Mech.* (2013) P04004; *J. Stat. Phys.* **153**, 289 (2013).
- [59] F. Ginelli, H. Hinrichsen, R. Livi, D. Mukamel, and A. Politi, *Phys. Rev. E* **71**, 026121 (2005).
- [60] J. Adamek, M. Keller, A. Senftleben, and H. Hinrichsen, *J. Stat. Mech.* (2005) P09002.
- [61] H. Hinrichsen, *J. Stat. Mech.* (2007) P07006.
- [62] P. W. Anderson and G. Yuval, *Phys. Rev. Lett.* **23**, 89 (1969).
- [63] D. Thouless, *Phys. Rev.* **187**, 732 (1969).
- [64] F. J. Dyson, *Commun. Math. Phys.* **21**, 269 (1971).
- [65] J. L. Cardy, *J. Phys. A: Math. Gen.* **14**, 1407 (1981).
- [66] M. Aizenman, J. Chayes, L. Chayes, and C. Newman, *J. Stat. Phys.* **50**, 1 (1988).
- [67] J. Slurink and H. Hilhorst, *Phys. A (Amsterdam, Neth.)* **120**, 627 (1983).
- [68] A. Bar and D. Mukamel, *Phys. Rev. Lett.* **112**, 015701 (2014).
- [69] D. Poland and H. A. Scheraga, *J. Chem. Phys.* **45**, 1456 (1966).
- [70] M. E. Fisher, *J. Chem. Phys.* **45**, 1469 (1966).
- [71] R. Blossey and J. O. Indekeu, *Phys. Rev. E* **52**, 1223 (1995).
- [72] M. E. Fisher, *J. Stat. Phys.* **34**, 667 (1984).
- [73] D. J. Gross, I. Kanter, and H. Sompolinsky, *Phys. Rev. Lett.* **55**, 304 (1985).
- [74] C. Toninelli, G. Biroli, and D. S. Fisher, *Phys. Rev. Lett.* **96**, 035702 (2006).
- [75] C. Toninelli, G. Biroli, and D. S. Fisher, *Phys. Rev. Lett.* **98**, 129602 (2007).
- [76] J. Schwarz, A. J. Liu, and L. Chayes, *Europhys. Lett.* **73**, 560 (2006).
- [77] Y. Y. Liu, E. Csóka, H. Zhou, and M. Pósfai, *Phys. Rev. Lett.* **109**, 205703 (2012).
- [78] W. Liu, B. Schmittmann, and R. Zia, *Europhys. Lett.* **100**, 66007 (2012).
- [79] R. K. P. Zia, W. Liu, and B. Schmittmann, *Phys. Procedia* **34**, 124 (2012).
- [80] L. Tian and D. N. Shi, *Phys. Lett. A* **376**, 286 (2012).
- [81] G. Bizhani, M. Paczuski, and P. Grassberger, *Phys. Rev. E* **86**, 011128 (2012).
- [82] M. Sheinman, A. Sharma, J. Alvarado, G. H. Koenderink, and F. C. MacKintosh, *Phys. Rev. Lett.* **114**, 098104 (2015).
- [83] A. Bar and D. Mukamel, *J. Stat. Mech.* (2014) P11001.
- [84] J.-Ch. Anglès d'Auriac *et al.*, *J. Phys. A: Math. Gen.* **35**, 6973 (2002); J.-Ch. Anglès d'Auriac, in *New Optimization Algorithms in Physics*, edited by A. K. Hartmann and H. Rieger (Wiley-VCH, Berlin, 2004).
- [85] P. W. Kasteleyn and C. M. Fortuin, *J. Phys. Soc. Jpn.* **46**, 11 (1969).
- [86] R. Juhász, H. Rieger, and F. Iglói, *Phys. Rev. E* **64**, 056122 (2001).
- [87] Y. Imry and S. K. Ma, *Phys. Rev. Lett.* **35**, 1399 (1975).